Cavitation density of superfluid helium-4 around 1 K

An Qu, A. Trimeche, J. Dupont-Roc, J. Grucker, and Ph. Jacquier
Laboratoire Kastler Brossel, ENS-PSL Research University, CNRS, UPMC-Sorbonne-Universités, Collège de France, 24 rue Lhomond, 75005 Paris, France

(Received 14 April 2015; revised manuscript received 10 June 2015; published 25 June 2015)

Using an optical interferometric method, the cavitation density of bulk superfluid helium at $T = 0.96$ K is measured and found to be $\rho_{cav} = 0.1338 \pm 0.0002$ g cm^{-3}. A well-established equation of state for liquid helium at negative pressures converts this to the cavitation pressure $P_{cav} = -5.1 \pm 0.1$ bars. This cavitation pressure is consistent with a model taking into account the presence of quantized vortices, but disagrees with previously published experimental values of P_{cav}.

DOI: 10.1103/PhysRevB.91.214115 PACS number(s): 67.25.D−

I. INTRODUCTION

Because helium is a model material at low temperature, its phase transitions have been studied in much detail. In particular, the stability limits of the liquid phase with respect to the solid phase at high pressure and to the gas phase at negative pressure have been studied experimentally and theoretically (see the review articles of Balibar *et al.* [1,2]). To avoid wall-induced nucleation of the new phase, experimental over- and under-pressures are produced in bulk liquid away from any surface using high-amplitude focused sound waves [3]. While the appearance of the new phase is easily detected optically, the measurement *in situ* of the local pressure at which nucleation occurs is a challenge. Estimations have been drawn either from the oscillation amplitude of the sound emitter combined with an estimation of the gain due to the focusing [4–6], or from extrapolating the liquid static pressure down to where a vanishingly small sound wave would produce cavitation [6]. However nonlinear effects in the sound wave propagation introduce uncertainties in both methods.

In 2010, our group introduced a time-resolved quantitative multiphase interferometric imaging technique [7] for measuring the density of a medium inside a sound wave with cylindrical symmetry. In 2012, this technique was successfully applied for density measurements in solid helium at 1 K in pressure swings below the equilibrium melting pressure [8]. We intended to implement the same technique to study metastable liquid at pressure above this melting pressure. In order to check the method in liquid helium, we decided to measure first the liquid density at which cavitation occurs around 1 K aiming at verifying the results of Ref. [6]. In this article, we present our result for the cavitation density. Previous experimental results were given as cavitation pressures. So an equation of state for liquid helium at negative pressures has to be used for comparison. Fortunately, various theoretical approaches [9–12] have produced quite similar equations of state. To our surprise, our density result converted to pressure does not quite agree with previous estimations. Thus we also reproduced the pressure extrapolation of Caupin and Balibar [6], and found a reasonable agreement with their data. After discussion of various sources of uncertainties in our measurements, we compare our results with various theoretical estimates of the cavitation pressure.

II. EXPERIMENTAL SETUP

The technique to measure the local density variations in focused acoustic waves has been described in previous articles [7,8]. Here is a brief reminder.

The experimental cell containing liquid helium is cooled in a cryostat with four optical ports. The working temperature can be regulated from 0.9 K to 2.1 K. In the experiment described in this paper, the temperature is fixed at $T = 0.96$ K. The cell is connected to a buffer volume at room temperature, so that the static pressure P_{st} is easily monitored with the help of a Keller X35 pressure sensor with an accuracy of ± 15 mbars. A hemispherical piezoelectric transducer (PZT) excites and focuses ultrasound waves in helium at the frequency 1.15 MHz of its first thickness vibration mode. The transducer inner diameter is 12 mm, and the thickness is 2 mm. In order to observe directly the acoustic focus, a small part, 0.9 mm in height, has been removed around the transducer rim. One side of the transducer is grounded and the other side is connected to the output of a RF amplifier driven by an arbitrary function generator (AFG). A detailed scheme is shown in Fig. 1.

The optical part of the setup is a Jamin interferometric imaging system with a pulsed Nd:YAG laser ($\lambda_o = 532$ nm) as a light source and a CCD camera for detection. The focal region is imaged onto the CCD camera with a magnification factor of 2 using an appropriate lens. The spatial resolution of the entire system is 20 μm [7], about 1/10 of sound wavelength $\lambda_s = 0.24$ mm. The CCD camera orientation is such that columns of pixels are parallel to the transducer axis. Lines of pixels are thus along a radius of the sound field. One arm of the interferometer passes through the acoustic focal region while the other crosses the cell in an unperturbed zone. The acoustic wave introduces a density variation that modulates the refractive index of helium (mainly in the acoustic focus) and hence gives rise to an optical phase shift between the two paths. A pair of phase plates is placed between the laser and the cell. One of these phase plates is mechanically controlled by a computer in order to add a known phase shift to the unperturbed ray. This added phase shift enables us to extract the phase shift due to the variation of the refractive index as we will see in the next section.

III. LOCAL DENSITY MEASUREMENT

Using the AFG, we can choose the time t with respect to the sound pulse triggering at which an image of the interference

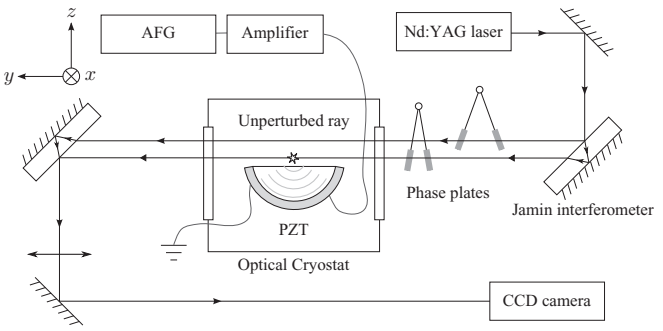

FIG. 1. Experimental setup. At the center of the transducer, the small star is the acoustic focus where cavitation occurs. A CCD camera monitors the focus plane through a lens. The camera image is composed of pixels distributed in lines and columns. We optimized the camera orientation so that lines are parallel to the x axis.

field is taken by the camera. This time is adjusted by steps of 0.05 μs, about 6% of the sound period. By repeating the measurements and recording images at successive delays on a relatively long period, we are able to reconstruct a temporal evolution of the interference field in the focal region.

The observed intensity of a given pixel at time t is expected to be

$$I(t) = I_0(t)\{1 + C(t)\cos[\delta\phi(t) + \beta]\}; \quad (1)$$

$\delta\phi(t)$ is the optical phase to be measured, and β is the controllable phase shift due to the phase plates. $I_0(t)$ and $C(t)$ are respectively the mean intensity and the fringe contrast. A series of measurements with different β at the same time enables us to extract the phases $\delta\phi(t)$ through a fit [7] of Eq. (1).

Let y be the light propagation axis, z the PZT axis, and x the axis orthogonal to y and z (Fig. 1). At a given delay t, the phase shift $\delta\phi(x,z)$ is related to the refractive index map by a simple integration along the y axis. In our case, the sound field is rotationally invariant around the hemisphere axis z, so that the refractive index variation δn is only a function of z and $r = \sqrt{x^2 + y^2}$. Given the fact that δn is 0 outside the sound field, we can write $\delta\phi$ as the Abel transform of δn:

$$\delta\phi(x,z) = \frac{2\pi}{\lambda}\int_{-\infty}^{+\infty} dy\, \delta n(\sqrt{x^2 + y^2}, z). \quad (2)$$

Conversely, radial refractive index profiles can be retrieved from phase shift maps via an inverse Abel transform. Then, using the Clausius-Mossotti relation in the limit $n_0 \sim 1$, the density variation $\delta\rho$ of the medium can be deduced easily:

$$\frac{\delta n}{n_0 - 1} = \frac{\delta\rho}{\rho_0}, \quad (3)$$

n_0 and ρ_0 being the unperturbed refractive index and density. From the measured quantity δn, the density itself is easily deduced by $\rho = \rho_0(1 + \frac{\delta n}{n_0 - 1})$. Figure 2 shows a typical density radial profile obtained for $P_{st} = 0.15$ bars at the time when the density is minimum at acoustic focus.

IV. DETERMINING THE CAVITATION VOLTAGE

Our measurement of local density by interferometry requires a completely reproducible phenomenon. If bubbles

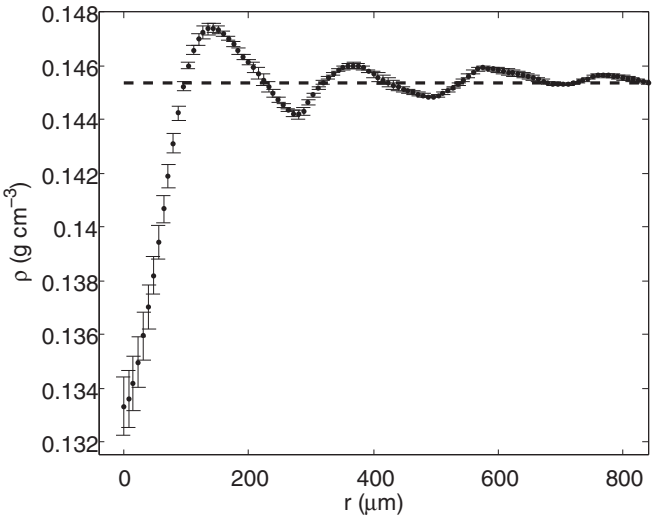

FIG. 2. Typical radial density profile for $P_{st} = 0.15$ bar at the time when the density is minimum at acoustic focus. The static density corresponding to P_{st} is shown by the horizontal dashed line. The error bar calculation is detailed in Sec. V.

appear randomly, it is impossible to measure the optical phase shift $\delta\phi(t)$ for the pixels involved. In other words, this method only allows us to measure the local density just below the cavitation density where no cavitation process occurs (or the cavitation probability is very low). Then the measured local density should be very close to the real cavitation density and a linear extrapolation to the cavitation voltage would introduce only a small correction.

Thus, before performing any density measurement, we have to precisely determine the cavitation voltage. Other groups have observed that bubble lifetime in superfluid helium depends on the static pressure P_{st} and is of the order of some tens of microseconds [4,13]. Then, $\sim$10 μs after the minimum pressure wave front passed the acoustic focus, bubbles have expanded to their maximum size and are easily observed on the CCD camera (see Fig. 3).

The cavitation process has a statistical behavior because of the thermal fluctuations. According to Caupin *et al.* [6], this probability is described by the "asymmetric S-curve formula":

$$\Sigma(V) = 1 - \exp\{-\ln 2\exp[\xi(V/V_c - 1)]\}, \quad (4)$$

where V is the excitation voltage, V_c the cavitation voltage, and ξ a dimensionless parameter. In order to determine V_c,

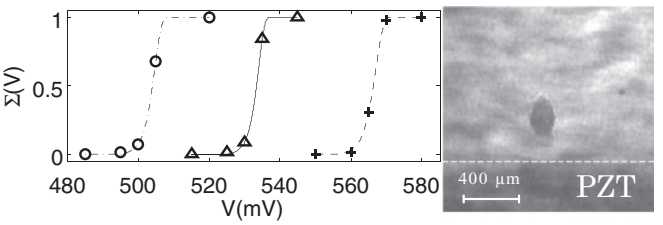

FIG. 3. Left: Cavitation probability at 0.96 K for three different pressures P_{st}: circles, 0.15 bars; triangles, 0.65 bars; crosses, 1.26 bars. The corresponding lines are fits according to Eq. (4). Right: Image of a bubble recorded by the camera 10 μs after its creation.

we proceed as follows. For a given static pressure, the bubble probability is determined for 5 different excitation voltages. Each voltage point corresponds to 1000 trials (1000 sound pulses) and the probability is then simply given by the number of positive events (creation of bubble) divided by the number of trials. The relative standard deviation on the probability is $1/\sqrt{1000} \simeq 3\%$. To avoid heating, 10 bursts of 100 sound pulses at 10 Hz repetition rate were shot, waiting 100 s between each burst. To precisely control the driving voltage of the PZT, we fixed the RF amplifier gain factor at about 390, and adjust only the AFG voltage amplitude with a relative accuracy of 10^{-4}. Hence we use the AFG voltage V as a scale to determine the cavitation voltage instead of the PZT driving voltage.

The cavitation voltage is the value corresponding to a bubble probability of $1/2$ according to Eq. (4). As can be seen in Fig. 3, the relative width of the curves is about 1% of V_c. These curves are indeed very sharp and for the AFG voltage $V_{\max}$ of about 2% below V_c, the probability $\Sigma(V_{\max})$ is about 10^{-3}.

V. CAVITATION DENSITY

In this section, we present our results for the cavitation density of superfluid helium at $T = 0.96$ K. The cavitation density was reached from three different static pressures : 0.15 bars, 0.65 bars, and 1.26 bars. For each static pressure, the cavitation voltage is determined following the approach depicted previously (see Fig. 3). Then the minimum density in time and space $\rho_{\min}$ was measured for several voltages below the cavitation threshold. An example is shown in Fig. 4. The density variation is not a linear function of the voltage. This is due to nonlinear effects in the acoustic wave and possibly to the appearance of shock waves [14]. Assuming a local linear dependence of $\rho_{\min}$ on V, and taking into account the error bars, one can safely consider ρ_{cav} is $\rho_{\min}(V_{\max})$. In order to improve the accuracy in determining ρ_{cav}, we have made a lot of measurements of the local density just below the cavitation voltage.

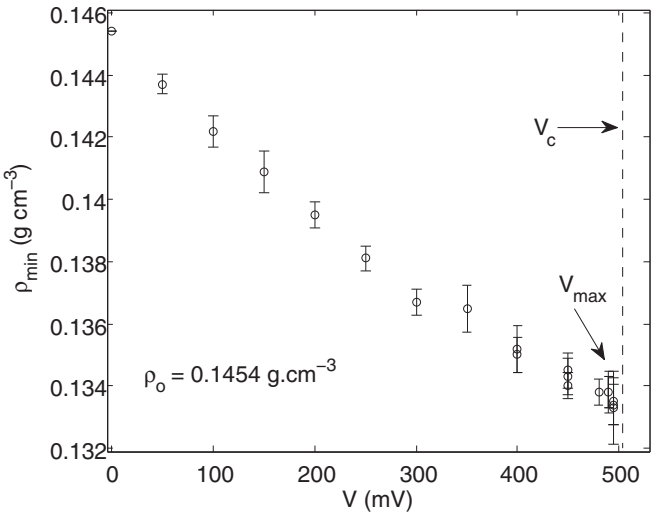

FIG. 4. Experimental measurements of minimum densities $\rho_{\min}$ for different driving voltages V at $T = 0.96$ K and $P_{st} = 0.15$ bars. The dashed line represents the cavitation voltage.

The measurement uncertainties can be divided in two parts: the statistical ones which come mainly from the extraction process of the optical phase shift induced by the acoustic wave, and the systematic errors arising from an imperfect cylindrical symmetry of the pressure wave.

As we mentioned earlier, for each time and for each pixel, the phase shift value $\delta\phi(t)$ is obtained by applying a fit on β-dependent intensities using Eq. (1) [7]. We use a computer program to extract these phases with 95% confidence bounds. This gives the phase shift uncertainties mainly due to shot noise, camera reading noise, and laser power fluctuations. Once the phase shift map is determined, an inverse Abel transform [7] is applied to recover the refractive index local variation induced by the acoustic wave. Then, the density variations are deduced from the optical index variations using Eq. (3). The inverse Abel transform is a linear transformation. In a given line of an image, which is along the x axis, the calculation of the optical index at a given pixel i depends linearly on the phase shift values for all pixels on the same line farther from the transducer axis. The local density variation at pixel i is thus in the form

$$\delta\rho_i = \sum_{j=i}^{j_{\max}} \alpha_{ij}\delta\phi_j, \tag{5}$$

where j is the pixel index in the line, α_{ij} is a weight, and $j_{\max}$ is the line end pixel where the sound field is negligible. The errors $\Delta\delta\rho_i$ on $\delta\rho_i$ can be computed from the error $\Delta\delta\phi_j$ on $\delta\phi_j$ and the weights α_{ij} which could be in principle extracted from the Abel inversion program. Instead we used a simpler empiric method, assuming that the phase uncertainty is about the same for each pixel, and is not correlated from one pixel to an other. In that case, the uncertainty of the density variation at the pixel i is

$$(\Delta\delta\rho_i)^2 = \sum_{j=i}^{j_{\max}} \alpha_{ij}^2(\Delta\delta\phi_j)^2 = (\Delta\delta\phi)^2 \sum_{j=i}^{j_{\max}} \alpha_{ij}^2. \tag{6}$$

Then, we performed $N = 1000$ density calculations, for the same treated line while adding a Gaussian noise to the phase shifts for every calculation. The standard deviation of the added noise is chosen to be the same as the phase shift uncertainty $\Delta\delta\phi$. Once we have these N treatments, the statistical uncertainty $(\Delta\delta\rho_i)_N$ of the radial density variation is calculated for each pixel of the line. By construction, this uncertainty is equal to $\sqrt{2}$ times the original unknown statistical uncertainty $\Delta\delta\rho_i$ of the density variation, because

$$(\Delta\delta\rho_i)_N^2 = \sum_{j=i}^{j_{\max}} \alpha_{ij}^2[(\Delta\delta\phi)^2 + (\Delta\delta\phi)^2] = 2(\Delta\delta\rho_i)^2. \tag{7}$$

Applying this method, we found that the statistical uncertainty around the cavitation density is on the order of 0.0002 g cm^{-3}, while the maximum value of $\delta\rho$ is of order 0.0125 g cm^{-3}.

The inverse Abel transform assumes that the symmetry axis is exactly known. Actually, it is unknown and has to be determined experimentally by searching a symmetry axis in the phase maps. But the noise in the phase as well as any possible asymmetry of the acoustic wave locally perturb the left-right symmetry of the phase shift maps. This perturbation will add

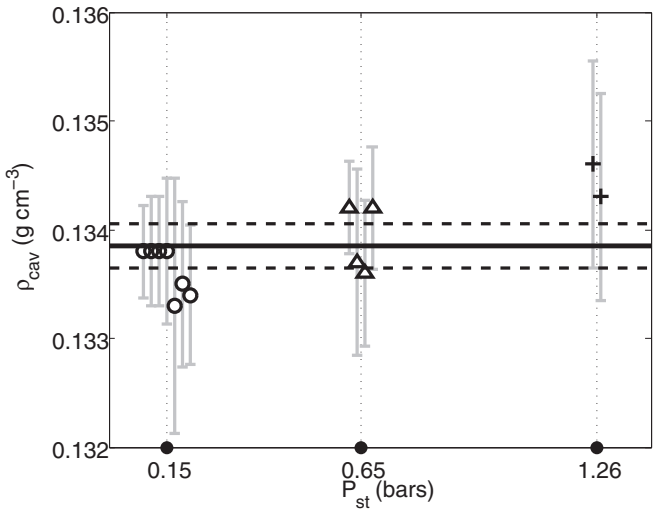

FIG. 5. Cavitation density as a function of static pressure at $T = 0.96$ K. For more clarity, the different measurements are shifted from their actual P_{st} values (black circles). The horizontal continuous line represents the average cavitation density and the dashed lines its uncertainty.

an uncertainty in the calculation of density variations. The difference between the Abel inversion applied to the left and to the right of this axis gives an order of magnitude of this uncertainty.

The symmetry axis for a given phase map is found by fitting a straight line through all symmetry centers when the amplitude of the sound pulse at focus is maximum. Then the mean and the standard deviations for the positions of these axis are computed. The uncertainty on the symmetry axis is about 3 μm, giving a contribution to the density variation uncertainty on the order of 0.0003 g cm^{-3}. To this systematic uncertainty we add another incertitude due to the difference between the left and right parts of the Abel inversion. This gap varies from one image to another and it is on the order of 0.0005 g cm^{-3}.

We have measured many minimum densities in the vicinity of the cavitation voltage at several static pressures (0.15 bars, 0.65 bars, and 1.26 bars) and at the same temperature 0.96 K as shown in Fig. 5. In this figure, the error bars represent the quadratic sum of statistical and systematic uncertainties for each minimum density measurement. Within the error bars we find as expected that ρ_{cav} is independent of P_{st}. Thus, we computed the mean of these measurements and their mean squared error to determine, respectively, the cavitation density of helium and its uncertainty. Our final result is that the cavitation density of superfluid helium-4 at 0.96 K is $\rho_{\mathrm{cav}} = 0.1338 \pm 0.0002$ g cm^{-3}.

Note that the uncertainty given here (2×10^{-4} g cm^{-3}) compared to the density variation $\delta\rho$ gives a relative uncertainty about 2%. Concerning the reliability of this measurement, it may be interesting to recall that a comparison with a hydrophone [7] was made in water in 2010. It was found that the deviation between the two methods is less than 5%.

VI. DISCUSSION

Previous results [5,6] about cavitation in liquid helium were given as cavitation pressures instead of cavitation densities. The equation of state (EOS) of liquid helium in its metastable state (density and pressure below the boiling curve values) is needed to convert the ρ_{cav} to a corresponding P_{cav}. Although such an equation of state has never been measured experimentally, some have been proposed. Maris has pointed out that, in the stable phase at $T = 0.1$ K, the sound velocity pressure dependence could be fitted very well by the law $c^3 = b(P - P_c)$ with c the sound velocity, P the pressure, P_c the spinodal pressure, and b a constant [15]. He proposed that this relationship holds in the metastable state (negative pressure). Bauer *et al.* have performed path-integral Monte Carlo simulations of liquid helium in the metastable state at finite temperature and found the same dependence of sound velocity on pressure [11]. Dalfovo *et al.* have calculated the EOS of metastable liquid helium at $T = 0$ K using a density functional approach [10], and Boronat *et al.* using a quadratic diffusion Monte Carlo method to achieve a similar EOS [9]. The EOSs at 0 K agree within a few percent. Moreover, using the density functional theory of Dalfovo *et al.*, Maris and Edwards have shown that in the temperature range $0 < T < 1$ K, the EOS is nearly independent of temperature [12].

So in order to compare our cavitation density result to cavitation pressure results of other experiments, we use the EOS for metastable liquid helium established in Ref. [15] and modified in Ref. [6] to correct for a unit error. This EOS is

$$P = P_s + \gamma(\rho - \rho_s)^3, \tag{8}$$

where the pressure P is in bars, the density ρ in g/cm^3, $P_s = -9.6435$ bars, $\gamma = 72\,904$ bars $(\mathrm{g/cm^3})^{-3}$, and $\rho_s = 0.094175$ g/cm^3. This equation is valid at $T = 0$ K and we assume it holds for $T = 0.96$ K [12]. Using this EOS, our cavitation pressure is $P_{\mathrm{cav}}(0.96\ \mathrm{K}) = -5.1 \pm 0.1$ bars.

At temperatures $\sim$1 K, in addition to the present experiment, there are to our knowledge only two experiments which studied the wall-induced free cavitation of liquid helium. Both also used focused acoustic wave. Xiong *et al.* [5] found that the cavitation pressure at 1 K is ~ -3 bars. The incertitude mentioned in this paper is about $\pm 10\%$ and comes mostly from the difficulty of estimating the pressure at acoustic focus knowing the displacement of the emitter. Nonlinear effects were not taken into account in their calculation. So this incertitude is likely to be underestimated. Caupin *et al.* [6] studied the dependence of cavitation voltage on the static pressure. They claim that this method enables them to set an upper limit for the actual cavitation pressure. Modeling a linear response of their emitter to voltage, they also give a lower limit for the cavitation pressure. Their result is $-9.8 < P_{\mathrm{cav}}(0.9\ \mathrm{K}) < -7.7$ bars. According to the data points published in [16], the result at $T \sim 1$ K is almost the same. One can see that there are large discrepancies among these experiments.

We have tried to reproduce the experiment of Caupin *et al.* using their extrapolation method on P_{st} [6] (see Appendix). The upper limit of P_{cav} we found is about -8 bars which agrees pretty well with the one of Caupin *et al.*. But the disagreement with our density measurement converted to pressure remains.

Jezek *et al.* [17] have calculated the cavitation pressure of liquid helium as a function of temperature, by using a density functional method and assuming the absence of

defects (especially vortices). In order to compute the cavitation pressure, the volume υ and the time τ in which nucleation is likely to occur are needed. We take $\upsilon = (\lambda_s/2)^3$ and $\tau = 0.1\ \mu$s is the $1/10$ of the sound period. This gives $\upsilon\tau \sim 10^{-13}$ cm^3 s. Using this $\upsilon\tau$ value, Jezek *et al.* calculated $P_{\rm cav}^{\rm Jezek}(0.96\ {\rm K}) \sim -6.9$ bars. This value is just between our result (-5.1 bars) and the central value (-8.8 bars) of Ref. [6].

Finally, we would like to point out that Maris has developed a model of cavitation in the presence of quantized vortices in liquid helium [18]. For a vortex density ranging from 10^4 to 10^{12} cm^{-2}, he finds that $-5.8 < P_{\rm cav}^{\rm vortices}(0.96\ {\rm K}) < -5.1$ bars. Although Maris cannot estimate the error bar on this simulation, we note that our result does lie in this range. Besides, Pettersen *et al.* [19] have proposed that the vortex density in the high-amplitude sound wave should be of the order of $10^8 \sim 10^{10}$ cm^{-2}. The presence of vortices might be a possible way to reconciliate our experimental result with simulations. Because vortices are very difficult to avoid in any experiment in superfluid helium, they are likely to be present also in other cavitation experiments and the experimental cavitation pressure should be similar to our value of $P_{\rm cav}$. Nevertheless, it remains to be understood why the extrapolation method of P_{st} of Ref. [6] seems to point towards the vortex free cavitation pressure rather than to the experimental value of $P_{\rm cav}$.

VII. CONCLUSION

Using an interferometric setup, we have measured the cavitation density of liquid helium-4 at $T = 0.96$ K and the result is $\rho_{\rm cav} = 0.1338 \pm 0.0002$ g/cm^3. Trying to compare this result with existing calculations on the cavitation pressure, we found that a model taking into account the presence of vortices in the liquid can rather satisfactorily explain our result. We plan to investigate the influence of vortices on cavitation in liquid helium in two ways. First, by studying the dependence of $\rho_{\rm cav}$ on temperature, a signature while crossing the lambda temperature should be seen. Second, we will probe the dependence on the density (in the metastable state) of the sound velocity and of the sound attenuation. This last part will be done using stimulated Brillouin scattering.

ACKNOWLEDGMENTS

We thank the Laboratoire Kastler Brossel mechanics workshop led by J. M. Isac for their support and especially O. S. Souramasing in making the PZT holder. Special thanks to S. Balibar and F. Caupin for lending us the RF amplifier and many helpful advices.

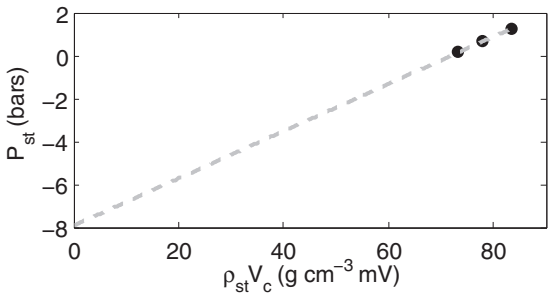

FIG. 6. Reproduction of Ref. [6] experiment. P_{st} as function of $\rho_{st} V_c$. The 3 data points (black circles) correspond to static pressures of 0.15 bars, 0.65 bars, 1.26 bars. Cavitation voltages are the ones shown in Fig. 3. The dotted line is the linear extrapolation of the data points.

APPENDIX: CAVITATION PRESSURE BY EXTRAPOLATING THE STATIC PRESSURE

In 2001, Caupin *et al.* implemented an extrapolation method [6] to investigate the behavior of helium in negative pressure. They imagined an environment with a "stable" negative static pressure. In this situation, the required driving voltage for achieving cavitation would be less than the one in null static pressure. Then the very negative static pressure corresponding to zero cavitation voltage would be the cavitation pressure. That can be expressed as

$$P_{\rm cav} = P_{\rm focus} = P_{st} + \Delta P(\rho_{st} V_c), \tag{A1}$$

where $P_{\rm cav}$, P_{st}, and $P_{\rm focus}$ are respectively the cavitation pressure, the static pressure of helium, and the pressure at acoustic focus. $\Delta P(\rho_{st} V)$ is the variation of pressure induced by the sound wave and ρ_{st} is the static density. This equation holds when the driving voltage V reaches cavitation voltage V_c. Assuming that the cavitation pressure is independent of P_{st}, we measure the different cavitation voltages at different static pressures, and then extrapolate linearly at zero cavitation voltage [20]. Numerical simulations [14] have shown that in the absence of vortices the true curve is concave toward negative pressures. The linear extrapolation gives an upper limit of the true cavitation pressure.

Figure 6 shows our extrapolation corresponding to our measurements of (P_{st}, V_c) values (see Fig. 3). The upper limit of cavitation pressure obtained in this way is -7.9 ± 0.3 bars. This is in agreement with Caupin *et al.*'s value.

[1] S. Balibar, Nucleation in quantum liquids, J. Low Temp. Phys. **129**, 363 (2002).

[2] S. Balibar and F. Caupin, Nucleation of crystals from their liquid phase, C. R. Phys. **7**, 988 (2006).

[3] One may be worried by the possible presence of heterogeneous nucleation centers inside the bulk liquid. Atomic or molecular impurities other than helium are frozen in the filling line of the experimental cell or on the walls of the cell itself. Isotopic ^{3}He impurities are present at the standard level of 0.3 ppm. They are unlikely to play a significant role in cavitation because of their atomic size, much smaller than the size of the critical nucleus for cavitation [15]. Another type of defect exists in superfluid helium, namely quantized vortices. Their possible effect is discussed in Sec. VI.

[4] J. A. Nissen, E. Bodegom, L. C. Brodie, and J. S. Semura, Tensile strength of liquid ^{4}He, Phys. Rev. B **40**, 6617 (1989).

[5] Q. Xiong and H. J. Maris, Study of cavitation in superfluid helium-4 at low temperatures, J. Low Temp. Phys. **82**, 105 (1991).

[6] F. Caupin and S. Balibar, Cavitation pressure in liquid helium, Phys. Rev. B **64**, 064507 (2001).

[7] F. Souris, J. Grucker, J. Dupont-Roc, P. Jacquier, A. Arvengas, and F. Caupin, Time-resolved multiphase interferometric of a highly focused ultrasound pulse, Appl. Opt. **49**, 6127 (2010).

[8] F. Souris, J. Grucker, J. Dupont-Roc, and P. Jacquier, Observation of metastable hcp solid helium, Europhys. Lett. **95**, 66001 (2011).

[9] J. Boronat, J. Casulleras, and J. Navarro, Monte Carlo calculations for liquid ^{4}He at negative pressure, Phys. Rev. B **50**, 3427 (1994).

[10] F. Dalfovo, A. Lastri, L. Pricaupenko, S. Stringari, and J. Treiner, Structural and dynamical properties of superfluid helium: A density-functional approach, Phys. Rev. B **52**, 1193 (1995).

[11] G. H. Bauer, D. M. Ceperley, and N. Goldenfeld, Path-integral Monte Carlo simulation of helium at negative pressures, Phys. Rev. B **61**, 9055 (2000).

[12] H. J. Maris and D. O. Edwards, Thermodynamic properties of superfluid ^{4}He at negative pressure, J. Low Temp. Phys. **129**, 1 (2002).

[13] S. Balibar, C. Guthmann, H. Lambare, P. Roche, E. Rolley, and H. Maris, Quantum cavitation in superfluid helium 4?, J. Low Temp. Phys. **101**, 271 (1995).

[14] C. Appert, C. Tenaud, X. Chavanne, S. Balibar, F. Caupin, and D. d'Humires, Nonlinear effects and shock formation in the focusing of a spherical acoustic wave, Eur. Phys. J. B **35**, 531 (2003).

[15] H. Maris, Theory of quantum nucleation of bubbles in liquid helium, J. Low Temp. Phys. **98**, 403 (1995).

[16] F. Caupin, S. Balibar, and H. J. Maris, Limits of metastability of liquid helium, Phys. B (Amsterdam, Neth.) **329-333**, 356 (2003).

[17] D. M. Jezek, M. Guilleumas, M. Pi, M. Barranco, and J. Navarro, Thermal nucleation and cavitation in ^{3}He and ^{4}He, Phys. Rev. B **48**, 16582 (1993).

[18] H. J. Maris, Nucleation of bubbles on quantized vortices in helium-4, J. Low Temp. Phys. **94**, 125 (1994).

[19] M. S. Pettersen, S. Balibar, and H. J. Maris, Experimental investigation of cavitation in superfluid ^{4}He, Phys. Rev. B **49**, 12062 (1994).

[20] Although we use the AFG generator voltage, it is strictly proportional to the real driving voltage so that the extrapolation result will not be affected.